

Direct Imaging of Ionic Aggregates in Zn-Neutralized Poly(ethylene-*co*-methacrylic acid) Copolymers

Jonathan H. Laurer and Karen I. Winey*

Laboratory for Research on the Structure of Matter,
Department of Materials Science and
Engineering, University of Pennsylvania,
Philadelphia, Pennsylvania 19104-6272

Received September 22, 1998

Revised Manuscript Received November 4, 1998

Introduction. Several models have been proposed to describe ionic aggregation in random ionomers and account for small-angle scattering results,^{1–7} although scattering data alone have been insufficient to prove or disprove the competing models. In many other areas of polymer science, electron microscopy, particularly transmission electron microscopy (TEM), has been able to elucidate the most appropriate morphological models.⁸ Unfortunately, electron microscopy has thus far failed to provide reliable information on the morphology of bulk random ionomers.⁹

Nanoscale, crystalline particles can routinely be imaged using TEM by positioning a particle in a Bragg condition and using diffraction contrast to generate an image. However, the nanoscale aggregates in ionomers are amorphous, which forces microscopists to rely on amplitude contrast to detect the aggregates. This presents an interpretive challenge, because the phase contrast (i.e. carbon grain) is similar in appearance, and thereby obscures the ionic aggregates.⁹ Attempts to augment the amplitude (i.e. mass–thickness) contrast in the image by using chemical stains have failed, because they are either insufficiently selective or create artifacts.⁹ Thus, we employ scanning transmission electron microscopy (STEM) which uses detectors to collect the intensity at each point to generate images without phase contrast. The two primary imaging modes in STEM are high-angle annular dark field (HAADF) and bright field (BF). HAADF STEM has the advantage that intensity increases with atomic number (Z),¹⁰ thus eliminating the need for chemical staining. Furthermore, to avoid changes in microstructure associated with solution preparation,^{9,11,12} we preserve the bulk morphology by cryomicrotoming thin sections of ionomers. To our knowledge this is the first report using STEM methods to image microtomed sections to accurately reflect the state of ionic aggregation in ionomers.

Materials and Methods. A poly(ethylene-*co*-methacrylic acid) (E/MAA) copolymer, synthesized by high-pressure free radical copolymerization of ethylene (85 wt %) and methacrylic acid (15 wt %), was supplied by DuPont along with two Zn-neutralized ionomers. These materials have ca. 20% crystallinity (determined via DSC) and are part of a family of semicrystalline ionomers examined by several previous researchers.^{4,13–16} The ionomers are identified as ZnXX, where XX is the neutralization level: Zn58 and Zn22 correspond to 1.6 and 0.6 mol % Zn, respectively. Thin sections were obtained using a Reichert-Jung Ultracut S ultramicrotome, maintained at -110°C . Scanning transmission electron microscopy (STEM) was performed on a JEOL 2010F field emission electron microscope operated at

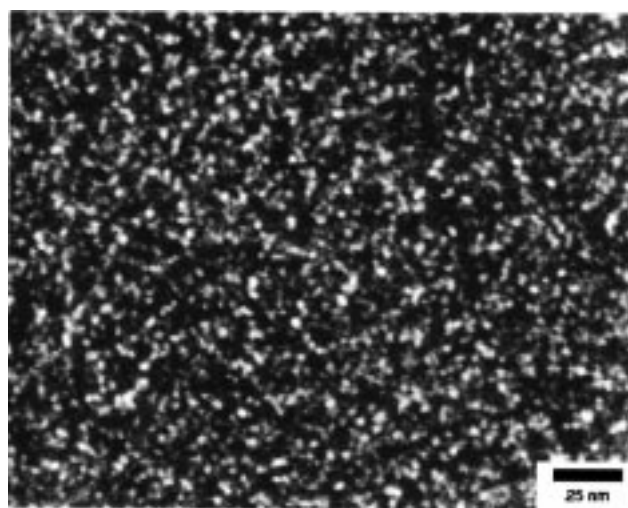


Figure 1. High-angle annular dark field (HAADF) STEM image of the Zn-neutralized ionomer Zn58, containing 1.6 mol % Zn. The Zn-rich aggregates appear as isotropic bright circles measuring $2.8 (\pm 0.5)$ nm in diameter, exhibiting narrow size polydispersity.

197 kV with a 1 cm STEM camera length and $50\text{ }\mu\text{m}$ condenser aperture. Images were collected using both high-angle annular dark field (HAADF) and bright field (BF) scintillating detectors.

Results and Discussion. An HAADF STEM image of the Zn58 ionomer is presented in Figure 1 and exhibits numerous bright domains. In HAADF STEM, or Z -contrast microscopy, the detected intensity varies with atomic number (Z), causing high- Z regions of the sample to appear bright.¹⁰ The bright domains in Figure 1 represent regions rich in Zn ($Z = 30$), because they possess a higher mean atomic number than the E/MAA matrix. (These particles do not diffract, so they cannot be attributed to excess ZnO, the neutralizing agent.) The Zn-rich domains exhibit uniform intensity and are nearly circular in projection. From the absence of rodlike or disklike projections and the isotropic nature of the specimen, we conclude that the aggregates are approximately spherical. The ionic aggregates also exhibit a narrow size distribution, having diameters of ca. $2.8 (\pm 0.5)$ nm. The section thicknesses produced by microtomy are more than 15 times the aggregate diameter, accounting for the overlapping aggregates in Figure 1. Thus, Figure 1 indicates that this bulk ionomer contains isotropic, spherical, Zn-rich ionic aggregates of narrow size distribution. Previous microscopy studies have reported far less uniformity, a likely result of using solution-cast thin films as opposed to microtomed sections of bulk sections.

Confirmation that the contrast observed in Figure 1 is due solely to the presence of Zn-rich ionic aggregates is provided by the HAADF STEM image of the unneutralized E/MAA copolymer in Figure 2. This image is characterized by a uniform gray level, which is consistent with a specimen of homogeneous composition. The lack of contrast also ensures that coherent (Bragg) scattering from ethylene crystals does not contribute to the HAADF signal at the camera length and geometry used.

The Zn22 ionomer is shown in the BF/HAADF image pair of Figure 3. In BF imaging, mass–thickness

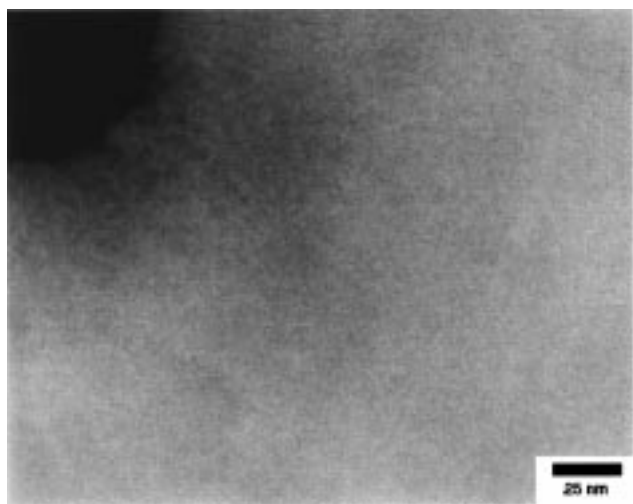


Figure 2. High-angle annular dark field (HAADF) STEM image of the E/MAA copolymer. The absence of features corresponds to a homogeneous distribution of the low- Z elements H, C, and O. The dark region in the upper left corner is a hole in the specimen (which appears dark in the HAADF imaging mode) and was used as a focal aid.

contrast dominates and high- Z domains appear dark, as when selective stains are used. When one changes from BF (Figure 3a) to HAADF (Figure 3b) on the same area of the Zn22 specimen, a one-to-one correspondence, or contrast reversal, is observed between dark and bright domains. These Zn-rich aggregates in Zn22 are the only features in either image, and have many features in common with Zn58: diameter $2.5 (\pm 0.5)$ nm, narrow size polydispersity, nearly circular projections, and isotropic spatial distribution. There are, however, significantly fewer domains per projected area in Zn22 than in Zn58; compare Figures 1 and 3b. The effect of increasing counterion concentration is to increase the number density of ionic aggregates, more so than to alter their size or shape. This behavior supports the concept that steric restrictions or charge screening by the matrix polymer determines aggregate size and shape.¹⁻³

The size of ionic aggregates in Figures 1 and 3 can be used to estimate the number of Zn ions per aggregate, n_{Zn} , when an aggregate composition is assumed. In terms of n_{Zn} , the number of each constituent in the aggregate may be written as

$$n_{\text{MAA}} = \nu n_{\text{Zn}} \quad (1)$$

$$n_{\text{PE}} = j n_{\text{MAA}} = j \nu n_{\text{Zn}} \quad (2)$$

where ν is the number of MAA units neutralized per Zn ion and j is the number of PE units per MAA unit in an aggregate. Assuming that the ionic aggregates are neutral, the charge on the counterion determines ν and in this study $\nu = 2$ for Zn^{2+} . The STEM results do not provide an independent measurement of j , so a range of aggregate compositions are considered, specifically, $j = 0-20$. Thus, the composition of the aggregates is given by the number ratio $n_{\text{Zn}}:n_{\text{MAA}}:n_{\text{PE}}$, which is $1:\nu:j\nu$. Using the bulk densities of these three constituents,¹⁷ the composition of the aggregates can be used to compute the aggregate density, ρ_{agg} , which depends on ν and j . The density of the aggregate can also be written as

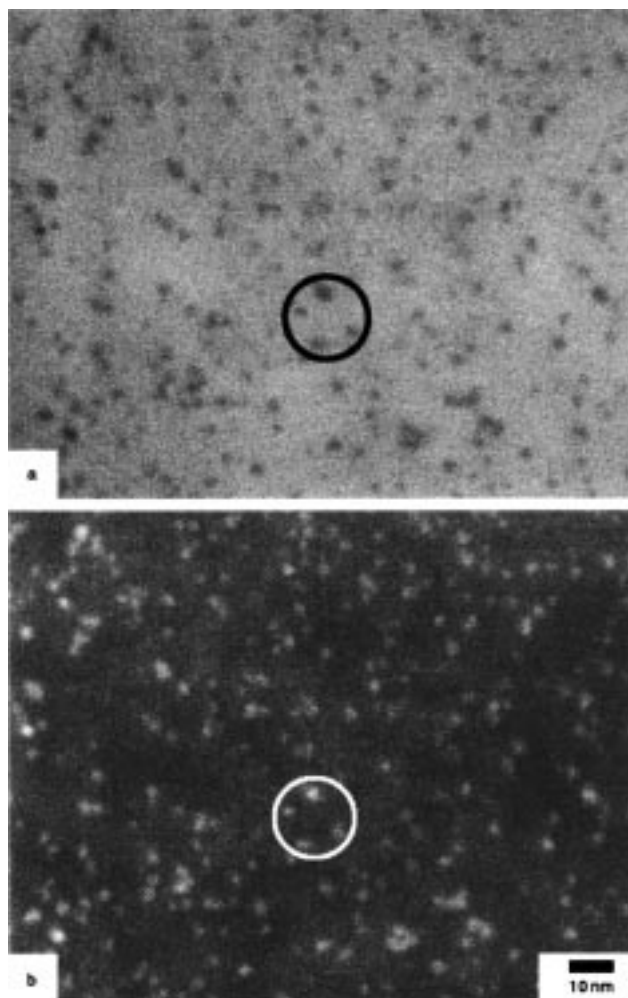


Figure 3. Bright field (BF) STEM image (a) and HAADF STEM image (b) of the same region of the Zn22 ionomer, containing 0.6 mol % Zn. In BF mode, the higher- Z domains appear dark. The same domains undergo contrast reversal when imaged in HAADF mode, but are otherwise invariant to imaging mode. This lends additional confirmation that the features do in fact represent Zn-rich aggregates. Like those of Zn58, the Zn-rich aggregates are isotropically distributed and have a narrow size polydispersity, measuring $2.5 (\pm 0.5)$ nm in diameter. The circles, enclosing a few representative domains, are provided to assist comparison of all features in both micrographs.

$$\rho_{\text{agg}} = \frac{m_{\text{Zn}} + m_{\text{MAA}} + m_{\text{PE}}}{V_{\text{agg}}} \quad (3)$$

where $m_i = n_i M_i$ (with $M_i = 65, 86$, and 28 g/mol for $i = \text{Zn}, \text{MAA}$, and PE , respectively) and V_{agg} is the volume of the aggregate which is determined experimentally. Combining eqs 1-3 provides an expression for the Zn-aggregation number:

$$n_{\text{Zn}} = \rho_{\text{agg}} V_{\text{agg}} [M_{\text{Zn}} + \nu M_{\text{MAA}} + j \nu M_{\text{PE}}]^{-1} \quad (4)$$

Calculations of ρ_{agg} and n_{Zn} are presented in Figure 4 for both Zn22 and Zn58 ionomers over a range of aggregate compositions, j . As expected, the Zn-aggregation number decreases significantly as the amount of the polymer chain within the aggregates increases. This analysis of the STEM images indicates that the Zn-aggregation number may be as high as 80 ions per aggregate for small values of j . Recall that this E/MAA copolymer has ca. 5.4 mol % MAA units, so that there

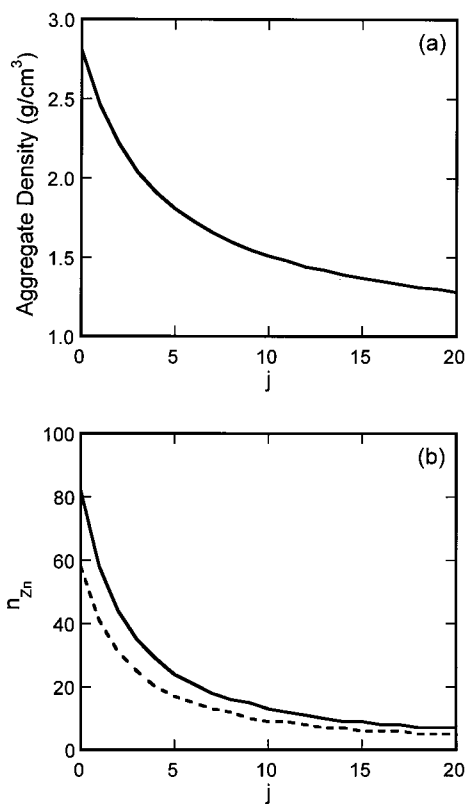


Figure 4. Calculated aggregate densities (a) and Zn-aggregation numbers (b), as a function of the number of PE units per MAA unit in the aggregate (j). In part b, the solid line corresponds to Zn58 ($D_{\text{agg}} = 2.8 \text{ nm}$), while the dashed line is for Zn22 ($D_{\text{agg}} = 2.5 \text{ nm}$).

are an average of 17 PE units between MAA units. However, the partial neutralization of the MAA units (22% or 58%) implies there are approximately 80 or 30 total monomer units between Zn–MAA complexes, respectively.

In the Eisenberg–Hird–Moore (EHM) multiplet-cluster model of amorphous ionomer morphology,² a multiplet is an aggregate of closest-packed counterions which excludes nonionic monomeric segments; in our notation this corresponds to $j = 0$. The multiplets proposed in the EHM model have the following characteristics: $D_{\text{agg}} \sim 0.6 \text{ nm}$; $n_{\text{ion}} \sim 5\text{--}10$. In contrast, the ionic aggregates we detect in semicrystalline ionomers are larger than the proposed multiplets by a factor of ~ 5 in size. For the aggregate composition corresponding to $j = 0$, our aggregation numbers are $\sim 60\text{--}80$, approximately 1 order of magnitude larger than predicted by EHM model for amorphous ionomers. Consequently, the observed ionic aggregates in these Zn-neutralized E/MAA semicrystalline ionomers are not isolated multiplets. Furthermore, the uniformity of contrast, shape and size of the observed Zn-rich aggregates indicates that these features are not likely to be assemblies of individual multiplets.

Other aggregation models have been proposed for random ionomers.^{1–7} In general, each model successfully describes a portion of the observed scattering behavior, but a single predictive model remains elusive. A critical evaluation of scattering results has been provided by Yarusso and Cooper.³ They propose a modified hard-sphere model and apply it primarily to amorphous Zn-neutralized sulfonated polystyrene (SPS) ionomers. At 23% and 53% neutralization, they find aggregate diam-

eters on the order of 2 nm .³ Increasing counterion content was found to increase the number of aggregates, with no significant change in diameter.^{3,4} While these findings are consistent with our STEM results, Yarusso and Cooper report much smaller aggregates for E/MAA ionomers similar to those examined in this report.⁴ Because the ionomer SAXS peak in E/MAA ionomers is relatively broad, they report that their model was more difficult to apply to this system.⁴ The STEM images presented herein provide model-independent evidence that Zn-aggregates in E/MAA ionomers are similar in size to those reported from SAXS studies of the Zn–SPS system.

Conclusions. Direct images of ionic aggregates in two Zn-neutralized E/MAA ionomers have been acquired using STEM in BF and HAADF modes. STEM avoids the shortcomings of previous imaging efforts and was applied to microtomed sections from the bulk specimens. Ionic aggregates were found to be randomly distributed and nearly spherical with a narrow size distribution. The size of the Zn-rich ionic aggregates are $2.5\text{--}2.8 \text{ nm}$ in diameter, with no significant change when the neutralization was increased from 22% to 58%. However, the number density of Zn-rich domains increased substantially with neutralization, in agreement with the experimental observations of Yarusso et al.^{3,4} On the basis of the observed domain size and a range of assumed aggregate compositions, the Zn-aggregation number for these ionic aggregates was determined to be in the range $5\text{--}80$. Our characterization of the Zn-rich ionic aggregates in the E/MAA systems is inconsistent with the proposed EHM model of multiplets in ionomers.

Acknowledgment. We thank Dr. John Van-alsten (DuPont) for materials and helpful discussion, and Dr. Rollin E. Lakis (LRSM) for technical assistance and support of the JEOL 2010F microscope. This work was supported by the following grants: DuPont Young Professor Grant, NSF-YIA (DMR 94-57997), and NSF–MRSEC (DMR 96-32598). The JEOL 2010F electron microscope was purchased by the LRSM with a grant from the NSF (DMR 94-13550).

References and Notes

- (1) Eisenberg, A. *Macromolecules* **1970**, *3*, 147.
- (2) Eisenberg, A.; Hird, B.; Moore, R. B. *Macromolecules* **1990**, *23*, 4098.
- (3) Yarusso, D. J.; Cooper, S. L. *Macromolecules* **1983**, *16*, 1871.
- (4) Yarusso, D. J.; Cooper, S. L. *Polymer* **1985**, *26*, 371.
- (5) Roche, E. J.; Stein, R. S.; Russell, T. P. *J. Polym. Sci., Polym. Phys. Ed.* **1980**, *18*, 1497.
- (6) Ding, Y. S.; Hubbard, S. R.; Hodgson, K. O.; Register, R. A.; Cooper, S. L. *Macromolecules* **1988**, *21*, 1698.
- (7) Marx, C. L.; Caulfield, D. F.; Cooper, S. L. *Macromolecules* **1973**, *6*, 345.
- (8) Sawyer, L. C.; Grubb, D. T. *Polymer Microscopy*; Chapman and Hall: New York, 1987.
- (9) Handlin, D. L.; MacKnight, W. J.; Thomas, E. L. *Macromolecules* **1981**, *14*, 795.
- (10) Pennycook, S. J. *Ultramicroscopy* **1989**, *30*, 58.
- (11) Williams, C. E.; Colliex, C.; Horion, J.; Jérôme, R. in *Multiphase Polymers: Blends and Ionomers*; Utracki, L. A., Weiss, R. A., Eds.; ACS Symposium Series 395; American Chemical Society: Washington, DC, 1989; p 439.
- (12) Li, C.; Register, R. A.; Cooper, S. L. *Polymer* **1989**, *30*, 1227.
- (13) Ostocka, E. P.; Kwei, T. K. *Macromolecules* **1968**, *1*, 403.
- (14) Yarusso, D. J.; Cooper, S. L. *Polymer* **1985**, *26*, 371.
- (15) Vanhoorne, P.; Register, R. A. *Macromolecules* **1996**, *29*, 598.
- (16) Quiram, D. J.; Register, R. A.; Ryan, A. J. *Macromolecules* **1998**, *31*, 1432.
- (17) Computed using $\rho_{\text{Zn}} = 7.13$, $\rho_{\text{MAA}} = 1.18$, and $\rho_{\text{PE}} = 0.96 \text{ g/cm}^3$.

MA981503G